3

Electromagnetic Wave Scattering from Material Objects Using Hybrid Methods

Adam Kusiek, Rafal Lech and Jerzy Mazur
Gdansk University of Technology, Faculty of Electronics, Telecommunications and Informatics
Poland

1. Introduction

Recent progress in wireless communication systems requires the development of fast and accurate techniques for designing and optimizing microwave components. Among such components we focus on the structures where a set of metallic and dielectric objects is applied. The investigation of such structures can be divided into two areas of interest. The first approach includes open problems, i.e. the electromagnetic wave scattering by posts arbitrarily placed in free space and illuminated by plane wave or Gaussian beam. In these problems the scattered field patterns of the investigated structures in near and far zones are calculated. Such structures are applied to the reduction of strut radiation of reflector antennas Kildal et al. (1996), novel PBG and EBG structures realized as periodical arrays Toyama & Yasumoto (2005); Yasumoto et al. (2004) and polarizers Gimeno et al. (1994). The second approach concerns closed problems, e.g. the electromagnetic wave scattering by posts located in different type of waveguide junctions or cavities. The main parameters describing these structures are the frequency responses or resonant and cut-off frequencies. The aforementioned waveguide discontinuities, as well as cylindrical and rectangular resonators, play important role in the design of many microwave components and systems. Rectangular waveguide junctions and circular cavities consisting of single or multiple posts are applied to filters Alessandri et al. (2003), resonators Shen et al. (2000), phase shifters Dittloff et al. (1988), polarizers Elsherbeni et al. (1993), multiplexers and power dividers Sabbagh & Zaki (2001).
One group of the developed techniques used to analyze scattering phenomena is a group of hybrid methods which combine those of functional analysis with the discrete ones Aiello et al. (2003); Arndt et al. (2004); Mrozowski (1994); Mrozowski et al. (1996); Sharkawy et al. (2006); Xu & Hong (2004). The advantage of this approach is that the complexity of the problem can be reduced, and time and memory efficiency algorithms can be achieved. The aforementioned methods are focused on objects located in free space Sharkawy et al. (2006); Xu & Hong (2004) or in waveguide junctions Aiello et al. (2003); Arndt et al. (2004); Esteban et al. (2002). Here the objects are enclosed in a finite region where the solution is obtained with the use of discrete methods such as finite element method (FEM) Aiello et al. (2003), finite-difference time-domain (FDTD) Xu & Hong (2004) or frequency-domain (FDFD) Sharkawy et al. (2006) methods and method of moments (MoM) Arndt et al. (2004); Xu & Hong (2004). In open problems Sharkawy et al. (2006); Xu & Hong (2004) the relation between the fields in the inner and outer regions is found by calculating the currents on the interface between the regions.

The total scattered field from a configuration of objects is obtained from the time domain analysis where the steady state is calculated Xu & Hong (2004) or from the iterative scattering procedure in the case of frequency domain solution Sharkawy et al. (2006). In closed problems Aiello et al. (2003); Arndt et al. (2004) the boundary Dirichlet conditions Aiello et al. (2003) or general scattering matrix (GSM) approach Arndt et al. (2004) are used to combine both of the investigated regions.
In this chapter we would like to describe a hybrid MM/MoM/FDFD/ISP method of analysis of scattering phenomena. In comparison to alternative methods Aiello et al. (2003); Arndt et al. (2004); Aza et al. (1998); Rogier (1998); Roy et al. (1996); Rubio et al. (1999); Sharkawy et al. (2006); Xu & Hong (2004) the presented approach allows one to analyze scattering from arbitrary set of objects which can be located both in free space or in waveguide junctions. In the presented method an equivalent cylindrical or spherical object, enclosing a single object or a set of objects, is introduced. At its surface the total incident and scattered fields are defined and used to determine the transmission matrix representation of the object Waterman (1971). Since the transmission matrix contains the information about the geometry and the boundary conditions of the structure, instead of analyzing the object or group of objects with arbitrary geometry the effective cylinders or spheres described by their transmission matrices are used. In this approach the transmission matrix representation of each single scatterer with simple or complex geometry is calculated with the use of analytical MM and MoM techniques or discrete FDFD technique, respectively. Utilizing the iterative scattering procedure (ISP) Elsherbeni et al. (1993); Hamid et al. (1991); Polewski & Mazur (2002) to analyze a set of scatterers allows to obtain the total transmission matrix defined on a cylindrical or spherical contour surrounding the considered configuration of objects. As the total transmission matrix does not depend on the external excitation, it is possible to utilize the presented approach to analyze a variety of both closed and open problems.
The presented here considerations are limited to the analysis of sets of objects homogenous in one dimension. The validity and accuracy of the approach is verified by comparing the results with those obtained from own measurements, derived from the analytical approach (defined for simple structures) and the commercial finite-difference time-domain (FDTD) simulator *Quick Wave 3D (QWED)* (n.d.).

2. Formulation of the problem

It is assumed that the arbitrary configuration of objects is illuminated by a known incident field (see Fig. 1(a)). The aim of the analysis is to determine the scattered field which is a result of this illumination. In the approach we assume the existence of an artificial cylindrical or spherical surface (surface $\mathcal{S}$) that encloses the analyzed set of objects. With this assumption we divide the structure into two regions of investigation: inner region and outer region. On the surface $\mathcal{S}$, that separates the regions, the incident and scattered field can be related by an aggregated transmission matrix $\overline{\overline{\mathbf{T}}}$ ($\overline{\overline{\mathbf{T}}}$-matrix) Waterman (1971) (see Fig. 1(b)). The values of the $\overline{\overline{\mathbf{T}}}$-matrix terms depend on the material and geometry properties (e.g. shape of the posts, location and orientation in space) and do not depend on the excitation. Therefore, the investigated configuration can be placed in any external region, and the outer fields can be combined with fields coming from the inner region. In particular $\overline{\overline{\mathbf{T}}}$-matrix approach can be easily applied to the analysis of open problems e.g. beam-forming structures or periodic structures. Moreover, it can be utilized in the analysis of closed structures e.g. waveguide filters or resonators.

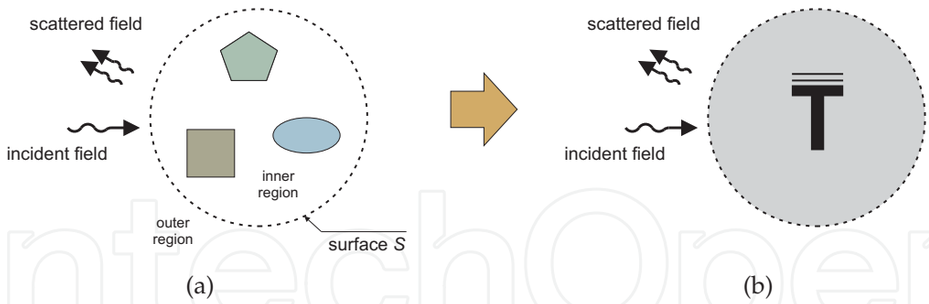

Fig. 1. Schematic representation of the analyzed problem: (a) multiple object configuration and (b) aggregated $\overline{\overline{\mathbf{T}}}$-matrix representation

In order to analyze the configuration of multiple objects placed arbitrarily in the inner region we utilize the analytical iterative scattering procedure (ISP) Elsherbeni et al. (1993); Hamid et al. (1991); Polewski & Mazur (2002). This method is based on the interaction of individual posts and allows to find a total scattered field on surface $\mathcal{S}$ from all the obstacles. This technique can be easily applied in orthogonal coordinate systems where the analytical solution of wave equation can be derived, e.g. cylindrical, elliptical or spherical coordinates. The ISP technique is thoroughly described in literature and previously was applied to the analysis of arbitrary sets of inhomogeneous height parallel cylinders Polewski & Mazur (2002) or arbitrary sets of spheres Hamid et al. (1991) (see Fig. 2). A more detailed description of the

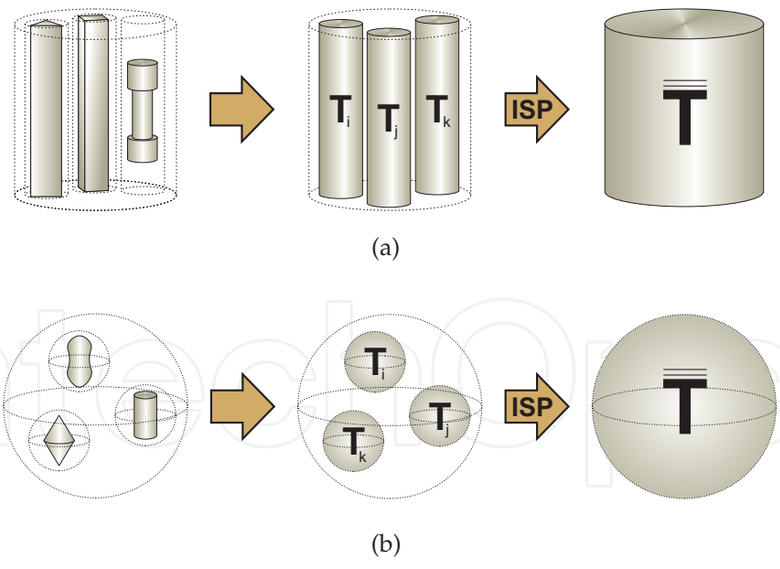

Fig. 2. Analytical iterative scattering procedure (ISP) defined in (a) cylindrical coordinates and (b) spherical coordinates

ISP will be presented in section 2.1
In order to generalize ISP to the configurations of objects with arbitrary geometry we employ different numerical techniques, depending on the post geometry. The basic concept of this approach is to enclose the analyzed object with irregular shape by the artificial homogeneous

cylinder or sphere (see Fig. 2). This allows us to utilize ISP formulated in cylindrical or spherical coordinates to determine aggregated transmission matrix $\overline{\overline{\mathbf{T}}}$ of the investigated configuration of posts with irregular shape.
We focus here on two groups of objects. One group includes cylinders with arbitrary cross-section and homogeneous along height and the other group includes axially symmetrical posts with irregular shape. The geometry properties of these objects allows one to simplify the three-dimensional (3D) problem to two-and-a-half-dimensional (2.5D) one which is more numerically efficient and less time-consuming. In the case of objects with

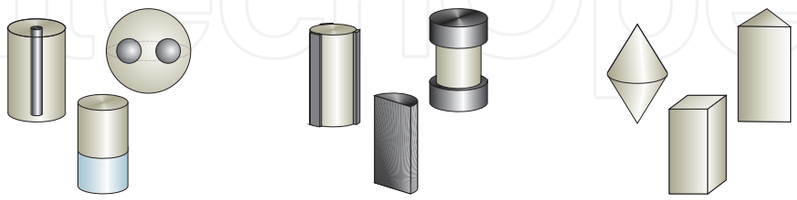

(a) (b) (c)

Fig. 3. Analyzed objects: (a) homogenous posts, (b) segments of cylinders and cylinders with conducting strips and (c) posts with irregular shape

simple geometry as presented in Fig. 3(a) the analytical mode-matching (MM) technique is utilized. In the case of objects presented in Fig. 3(b), e.g. metallized cylinders, fragments of metallic cylinders or corrugated posts the method of moments (MoM) is used. Finally, in the analysis of objects with irregular shape such as cylinders with arbitrary cross-section and axially-symmetrical posts shown in Fig. 3(c) the hybrid finite-difference frequency-domain/mode-matching (FDFD-MM) technique is applied. The aim of the single object analysis is to determine its own isolated transmission matrix **T** (**T**-matrix). All the mentioned techniques and **T**-matrix expressions for chosen types of posts will be presented in section 2.2.

2.1 Iterative Scattering Procedure

The ISP method is based on the interaction of individual posts and assumes that the incident field on a single post in one iteration is derived from the scattered field from the remaining posts in the previous iteration. In order to describe the ISP we assume that the analyzed configuration is composed of set of K objects located arbitrarily in global coordinate system xyz. Each analyzed object is represented by its transmission matrix $\mathbf{T}_i$ (where $i = 1, \ldots, K$). In the homogeneous region around the investigated post configuration we define the artificial cylindrical or spherical surface $\mathcal{S}$. The aim of analysis is to determine the relation between incident and scattered fields in the outer region on the surface $\mathcal{S}$.
In the first step we assume that objects are illuminated by an unknown incident field $F^{inc(0)}$ defined in global coordinate system. Depending on the formulation of the method these fields are defined as infinite series of cylindrical or spherical eigenfunctions with unknown coefficients. As the excitation wave illuminates all the posts inside the inner region, it has to be transformed from global coordinates of the inner region to the local coordinates of each object (see Fig. 4). As a result of this excitation a zero order scattered field $F_i^{scat(0)}$ from each post is created (see Fig. 5). The scattered field $F_i^{scat(0)}$ is defined in local coordinates $x_i y_i z_i$ and can be derived for desired excitation with the use of transmission matrix $\mathbf{T}_i$. Next the

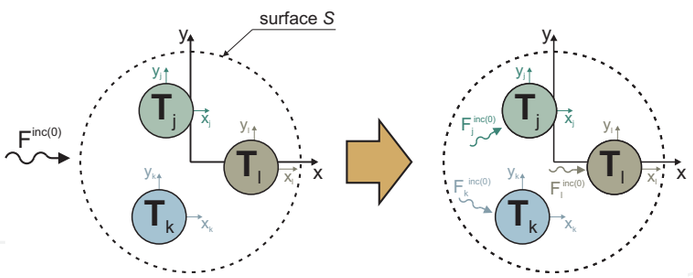

Fig. 4. Incident field $F^{inc(0)}$ transformation from global coordinates xyz to local coordinates $x_i y_i z_i$.

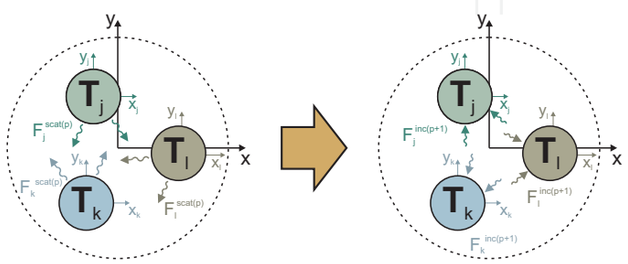

Fig. 5. Determination of new incident field in $(p+1)$th iteration based on the scattered field in pth iteration.

scattered field from the previous iteration coming from $K-1$ objects is assumed to be a new incident field $F_i^{inc(1)}$ on ith object in first iteration (see Fig. 5) and is defined as follows:

$$F_i^{inc(1)} = \sum_{\substack{j=1 \\ j \neq i}}^{K} F_{ij}^{inc(0)}, \tag{1}$$

where: $F_{ij}^{inc(0)}$ is a scattered field from jth object in zero iteration transformed to local coordinates $x_i y_i z_i$. Once again we derive the scattered field $F_i^{scat(1)}$ for each ith object in the configuration.
During the iteration process the scattered field from the previous iteration (from K-1 posts) is utilized as a new incident field on the remaining post and the coefficients of the pth iteration depend only on the coefficients of the $(p-1)$th iteration.
Using this method, after a sufficient number of iterations P, the scattered electric and magnetic fields from the ith post F_{Ti}^{scat} in its local coordinates are obtained as a superposition of the scattered fields from each iteration (see Fig. 6)

$$F_{Ti}^{scat} = \sum_{p=1}^{P} F_i^{scat(p)}. \tag{2}$$

Having transformed the scattered fields from the local coordinates of each post to the global coordinate system, one can define the total scattered field on the surface $\mathcal{S}$ as a superposition of the scattered fields from all K posts (see Fig. 6)

$$F_T^{scat} = \sum_{i=1}^{K} F_{T(i)}^{scat}. \tag{3}$$

Bearing in mind that the scattered field obtained during the iteration process depends on the

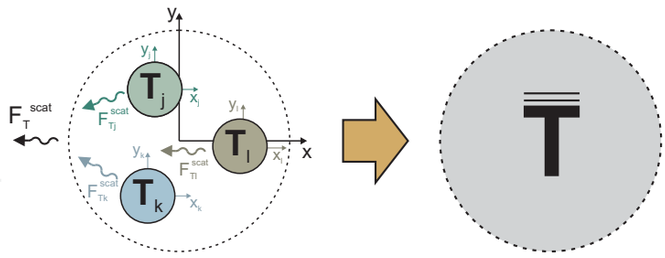

Fig. 6. Aggregated transmission matrix $\overline{\overline{\mathbf{T}}}$ of investigated objects configuration

unknown coefficients of zero order incident field, the investigated configuration of posts can be described by aggregated $\overline{\overline{\mathbf{T}}}$-matrix (see Fig. 6) defined in global coordinates xyz.
It should be emphasized that the described above analytical ISP allows one for fast and numerically efficient calculations of scattering parameters of arbitrary configuration of objects. In this approach the field transformation (interaction) matrices are evaluated only once for desired frequency and used in all iterations. Moreover, in each iteration the scattered fields from each post are obtained by simple multiplication and summation of matrices that makes this procedure numerically very efficient.

2.2 Single object analysis

In the single object analysis we try to describe the analyzed object by its isolated transmission matrix $\mathbf{T}$ defined on the surface S of the artificial cylinder or sphere which surrounds the object (see Figs. 7(a) and 7(b)). The introduction of this artificial surface $\mathcal{S}$ allows us to divide the computation domain into two regions: region I - inside the surface $\mathcal{S}$ and region II - outside the surface $\mathcal{S}$. The general solution of Helmholtz equation in cylindrical or spherical coordinates

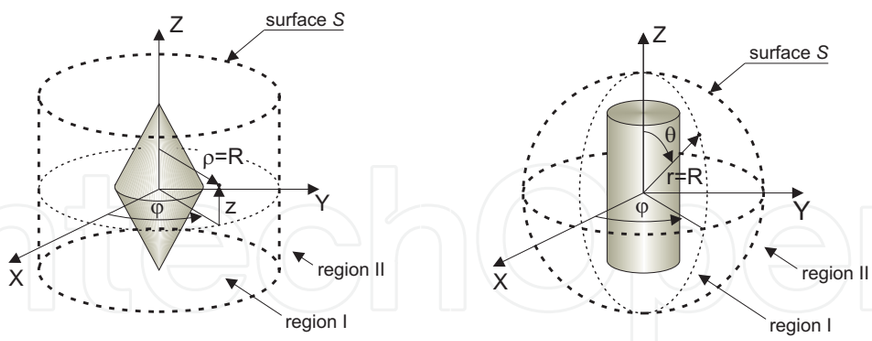

Fig. 7. Formulation of the problem for single object with irregular shape in: (a) cylindrical coordinates and (b) spherical coordinates.

in region II takes the following form:

$$E_t(\alpha,\beta,\gamma) = \sum_{k=1}^{2}\sum_{n=-\infty}^{\infty}\sum_{m=-\infty}^{\infty} A_{knm}^{E} f_{knm}^{\alpha}(\alpha) f_m^{\beta}(\beta) f_n^{\gamma}(\gamma), \tag{4}$$

$$H_t(\alpha,\beta,\gamma) = \sum_{k=1}^{2}\sum_{n=-\infty}^{\infty}\sum_{m=-\infty}^{\infty} A^H_{knm} f^{\alpha}_{knm}(\alpha) f^{\beta}_{m}(\beta) f^{\gamma}_{n}(\gamma), \tag{5}$$

where $f^{\alpha}_{k}(\alpha)$ determines the variation of the fields in direction normal to the surface $\mathcal{S}$ and $f^{\beta}_{m}(\beta) f^{\gamma}_{n}$ determines the variation of the fields in directions tangential to the surface $\mathcal{S}$. Variables α, β, γ denotes ρ, φ, z in cylindrical coordinates and r, φ, θ in spherical coordinates. In above equations field expansion coefficients A_{1nm} and A_{2nm} can be related with the use of isolated transmission matrix $\mathbf{T}$ as follows:

$$\mathbf{A}_2 = \mathbf{T}\mathbf{A}_1, \tag{6}$$

where $\mathbf{A}_1$ and $\mathbf{A}_2$ are the column vectors of A^E_{1nm}, A^H_{1nm} and A^E_{2nm}, A^H_{2nm}, respectively. In order to determine the transmission matrix of artificial cylinder or sphere containing analyzed post with irregular shape different techniques can be used as described in sections 2.2.1-2.2.2.

2.2.1 Analytical techniques

Transmission matrix $\mathbf{T}$ of homogeneous material cylinder can be simply evaluated using mode-matching technique. In this approach in each considered region the fields are expressed as series of eigenfunctions with unknown expansion coefficients. In order to eliminate the unknown coefficients in region 1 of the structure and to determine the relation between coefficients in the region 2 we need to satisfy the boundary conditions at the surface of the object. As a result we are obtaining the desired transmission matrix of the object. In the case of some material cylinders we present the form of transmission matrix $\mathbf{T}$ below. For the sake of brevity our considerations are limited to TM case.

- **metallic cylinder of radius** r

  The metalic cylinders find the application in structures where the high reflection coefficient is needed, e.g. microwave filters, power dividers and polarizers. The transmission matrix of such posts is defined as follows:

$$\mathbf{T} = \mathrm{diag}\left(-\frac{J_m(k_0 r)}{H^{(2)}_m(k_0 r)}\right)_{m=-M}^{m=M}, \tag{7}$$

  where $J_m(x)$ and $H^{(2)}_m(x)$ are Bessel and the second kind Hankel functions, respectively, of order m, and $k_0 = \omega\sqrt{\mu_0\varepsilon_0}$.

- **dielectric cylinder of radius** r **and relative permittivity** ε_r

  The dielectric cylinders are commonly utilized as different types of resonators in microwave structures. Their transmission matrix is defined as follows:

$$\mathbf{T} = \mathrm{diag}\left(\frac{k_0 J_m(kr) J'_m(k_0 r) - k_0 J'_m(kr) J_m(k_0 r)}{k J'_m(kr) H^{(2)}_m(k_0 r) - k_0 J_m(kr) H'^{(2)}_m(k_0 r)}\right)_{m=-M}^{m=M}, \tag{8}$$

  where $k = \omega\sqrt{\mu_0\varepsilon_0\varepsilon_r}$ and prime denotes a first derivative of the function with respect of the argument.

- **ferrite cylinder of radius** r **and tensor permeability** μ

  The ferrite cylinders are used in many microwave nonreciprocal devices such as circulators, isolators and phase shifters. The nonreciprocal properties can be controlled

by the direction and value of bias magnetization field. For the ferrite cylinder case the constitutive equations are expressed as follows:

$$\mathbf{D} = \varepsilon_0 \varepsilon_f \mathbf{E}, \tag{9}$$

$$\mathbf{B} = \mu_0 \boldsymbol{\mu} \mathbf{E}, \tag{10}$$

We assume that tensor $\boldsymbol{\mu}$ has the following dyadic form:

$$\boldsymbol{\mu} = \mu(\mathbf{i}_\rho \mathbf{i}_\rho + \mathbf{i}_\varphi \mathbf{i}_\varphi) + j\mu_a(\mathbf{i}_\rho \mathbf{i}_\varphi - \mathbf{i}_\varphi \mathbf{i}_\rho) + 1\mathbf{i}_z \mathbf{i}_z \tag{11}$$

with $\mu = 1 + \frac{p\delta}{\delta^2 - 1}$, $\mu_a = \frac{p}{\delta^2 - 1}$, $\delta = \frac{\gamma H_i}{f}$, $p = \frac{\gamma M_s}{f}$, H_i denotes internal bias magnetic field intensity, M_s saturated magnetization and γ gyromagnetic coefficient of the ferrite. For lossy ferrite $\delta = \delta_0 + j\alpha$ where $\delta_0 = \frac{\gamma H_i}{f}$, $\alpha = \frac{\gamma \Delta H}{f}$ and ΔH denotes resonance linewidth of ferrite.

Therefore, the **T**-matrix for the ferrite cylinder is defined as:

$$\mathbf{T} = \operatorname{diag}\left(\frac{k_0 J_m(kr) J'_m(k_0 r) - J_m(k_0 r)\left[\frac{k}{\mu_{eff}} J'_m(kr) - \frac{m}{r}\frac{\mu_a}{\mu_{eff}} J_m(kr)\right]}{H_m^{(2)}(k_0 r)\left[\frac{k}{\mu_e ff} J'_m(kr) - \frac{m}{r}\frac{\mu_a}{\mu_{eff}} J_m(kr)\right] - k_0 J_m(kr) H_m'^{(2)}(k_0 r)} \right)_{m=-M}^{m=M}. \tag{12}$$

where ε_f and $\mu_{eff} = \frac{\mu^2 - \mu_a^2}{\mu}$ denotes relative ferrite permittivity and effective ferrite permeability.

- **pseudo-chiral cylinders**

  Pseudo-chiral medium cylinders in spite of its isotropic nature allows to control the field distribution by changing the sign of pseudo-chiral admittance (direction of Ω particles in the post).

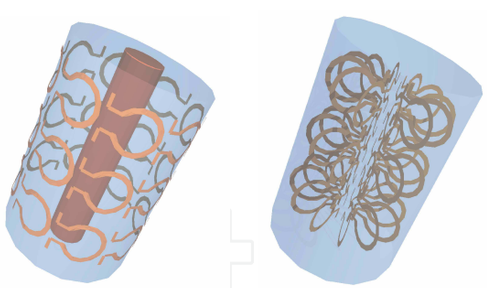

(a) (b)

Fig. 8. 3D view of a psuedo-chiral cylinders:
(a) type '1' and (b) type '2'

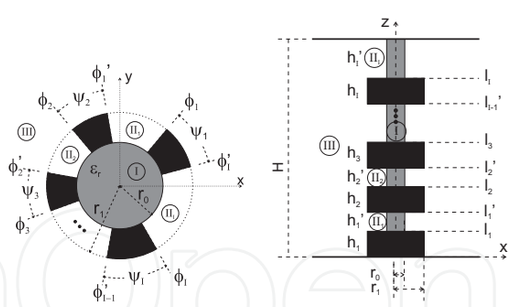

(a) (b)

Fig. 9. General configuration of the posts:
(a) metallized dielectric, (b) corrugated cylinder

  – **type '1'**

    For this case the Ω particles are arranged in the cylinder as shown in Fig. 8(a). Assuming the TM^z excitation and homogeneity of the field along z the constitutive equations are of the form:

$$\mathbf{D} = \varepsilon_0 \boldsymbol{\varepsilon} \mathbf{E} + j\boldsymbol{\Omega}_{\rho z} \mathbf{B}_\rho, \tag{13}$$

$$\mathbf{B} = \mu_0 \boldsymbol{\mu} \mathbf{H} - j\mu_0 \mu \boldsymbol{\Omega}_{\rho z} \mathbf{E}_z, \tag{14}$$

where $\boldsymbol{\varepsilon}$, $\boldsymbol{\mu}$ and $\boldsymbol{\Omega}$ are given in a dyadic form as:

$$\boldsymbol{\varepsilon} = \varepsilon \mathbf{i}_\rho \mathbf{i}_\rho + \varepsilon \mathbf{i}_\varphi \mathbf{i}_\varphi + \varepsilon_z \mathbf{i}_z \mathbf{i}_z, \tag{15}$$

$$\boldsymbol{\mu} = \mu_\rho \mathbf{i}_\rho \mathbf{i}_\rho + \mu \mathbf{i}_\varphi \mathbf{i}_\varphi + \mu \mathbf{i}_z \mathbf{i}_z \tag{16}$$

and $\boldsymbol{\Omega_{z\rho}} = \Omega \mathbf{i}_z \mathbf{i}_\rho$, $\boldsymbol{\Omega_{\rho z}} = \Omega \mathbf{i}_\rho \mathbf{i}_z$, Ω denotes pseudo-chiral admittance, $\varepsilon_z > \varepsilon$, $\mu_\rho > \mu$ and ε, μ are the parameters of a host medium where ε_z, μ_ρ depend on Ω. For $\Omega = 0$, $\varepsilon_z \longrightarrow \varepsilon$ and $\mu_\rho \longrightarrow \mu$.
For this case the **T**-matrix is defined as follows:

$$\mathbf{T} = \text{diag} \begin{pmatrix} J_m(k_0 r^{(2)}) X_v' - k_0 J_m'(k_0 r^{(2)}) X_v \\ k_0 H_m'^{(2)}(k_0 r^{(2)}) X_v - H_m^{(2)}(k_0 r^{(2)}) X_v' \end{pmatrix}_{m=-M}^{m=M}, \tag{17}$$

where: $X_v = J_v(k^{(2)} r^{(2)}) + A_v Y_v(k^{(2)} r^{(2)})$, $X_v = J_v(k^{(2)} r^{(2)}) + A_v Y_v(k^{(2)} r^{(2)})$ and A_v has the following form for dielectric and metallic inner core, respectively:

$$A_v = \frac{k^{(1)} J_v(k^{(2)} r^{(1)}) J_m'(k^{(1)} r^{(1)}) - k^{(2)} J_v'(k^{(2)} r^{(1)}) J_m(k^{(1)} r^{(1)})}{k^{(2)} Y_v'(k^{(2)} r^{(1)}) J_m(k^{(1)} r^{(1)}) - k^{(1)} Y_v(k^{(2)} r^{(1)}) J_m'(k^{(1)} r^{(1)})}, \tag{18}$$

$$A_v = -\frac{J_v(k^{(2)} r^{(1)})}{Y_v(k^{(2)} r^{(1)})}. \tag{19}$$

The prime symbol denotes the derivative with respect to argument.

– **type '2'**
For this case the Ω particles are arranged in the cylinder as shown in Fig. 8(b). Assuming the TM^z excitation and homogeneity of the field along z the constitutive equations are of the form:

$$\mathbf{D} = \varepsilon_0 \boldsymbol{\varepsilon_c} \mathbf{E} + j \boldsymbol{\Omega_{z\phi}} \mathbf{B}, \tag{20}$$

$$\mathbf{B} = \mu_0 \boldsymbol{\mu_c} \mathbf{H} - j \mu_0 \boldsymbol{\mu_c} \boldsymbol{\Omega_{\phi z}} \mathbf{E}. \tag{21}$$

The relative electric permittivity and magnetic permeability have dyadic form:

$$\boldsymbol{\varepsilon_c} = \varepsilon(\mathbf{i}_\rho \mathbf{i}_\rho + \mathbf{i}_\phi \mathbf{i}_\phi) + \varepsilon_z \mathbf{i}_z \mathbf{i}_z, \tag{22}$$

$$\boldsymbol{\mu_c} = \mu(\mathbf{i}_\rho \mathbf{i}_\rho + \mathbf{i}_z \mathbf{i}_z) + \mu_\phi \mathbf{i}_\phi \mathbf{i}_\phi. \tag{23}$$

The coupling dyadics are defined as $\boldsymbol{\Omega_{z\phi}} = \Omega_c \mathbf{i}_z \mathbf{i}_\phi$ and $\boldsymbol{\Omega_{\phi z}} = \Omega_c \mathbf{i}_\phi \mathbf{i}_z$.
T-matrix for this type of object has the following form:

$$\mathbf{T} = \text{diag} \left(\frac{P_v'^{(a)}(k_\rho r) J_m(k_0 r) - k_0 \eta_0 \mu_\phi \Omega_c P_v^{(a)}(k_\rho r) J_m(k_0 r) - \mu_\phi P_v^{(a)}(k_\rho r) J_m'(k_0 r)}{\mu_\phi P_v^{(a)}(k_\rho r) H_m^{(2)'}(k_0 r) - P_v'^{(a)}(k_\rho r) H_m^{(2)}(k_0 r) + k_0 \eta_0 \mu_\phi \Omega_c P_v^{(a)}(k_\rho r) H_m^{(2)}(k_0 r)} \right)_{m=-M}^{m=M} \tag{24}$$

where $P_v^{(a)}(\xi)$ is of the form:

$$P_v^{(a)}(\xi) = \sum_{n=0}^{\infty} c_n \xi^{n+\nu}. \tag{25}$$

where c_0 is an arbitrary constant, $c_1 = \dfrac{a c_0}{2\nu + 1}$ and $c_n = \dfrac{a c_{n-1} - c_{n-2}}{n(2\nu + n)}$ for $n \geq 2$. Selecting $c_0 = \dfrac{1}{2^\nu \Gamma(\nu + 1)}$, $P_v^{(a)}(\xi)$, amounts to Bessel function of the first kind when $\Omega_c = 0$ $(a = 0)$.

- **metallized or corrugated cylinder**

  The object with nonhomogeneous cross-section allows to modify the scattering parameters of the structures by the means of its simple rotation or vertical displacement. This property can be utilized in such structures as tunable filters, resonators or antenna beam-forming structures. This group includes the objects presented in Fig. 9. In order to find **T**-matrix of these structures we use the procedure that departs from standard mode-matching technique, and instead assumes the tangential component of electric field at the interface between regions of the structure by an unknown function $U(\phi)$ or $W(z)$. The functions $U(\cdot)$ and $W(\cdot)$ are then expanded in a series of basis functions with unknown coefficients. With this assumption, an additional degree of freedom is introduced in the problem. In other words, the introduction of the functions $U(\cdot)$ and $W(\cdot)$ allows to include in the formulation whatever information we have on the tangential electric field at the interface. The basis functions should contain as much of the a priori information we have on the behaviour of the tangential electric field at the interface as possible, its conditions at the sharp metallic edges of the ridge especially. A set of basis functions satisfying this local requirement is given as follows:

$$U_k^{(i)}(\phi) = \frac{f\left(\frac{k\pi(\phi-\phi_i)}{2(\pi-\theta_i)}\right)}{\sqrt[3]{(\phi-\phi_i)\left[2(\pi-\theta_i)-(\phi-\phi_i)\right]}} \quad i = 1, 2 \ldots I \tag{26}$$

$$W_k^{(i)}(z) = \frac{g\left(\frac{k\pi(z-l_i)}{h_i'}\right)}{\sqrt[3]{(z-l_i)(l_i'-z)}} \quad i = 1, 2 \ldots I-1 \tag{27}$$

$$W_k^{(I)}(z) = \frac{g\left(\frac{k\pi(z-l_I)}{2h_I'}\right)}{\sqrt[3]{(z-l_I)(2(H-l_I)-(z-l_I))}} \tag{28}$$

  where $f(\cdot)$ and $g(\cdot)$ are $\sin(\cdot)$ or $\cos(\cdot)$ functions and $2\theta_i = 2\pi - (\phi_i' - \phi_i)$.

  The inclusion of the information about the edge conditions at each of the metallic edges of the ridge allows for an efficient and accurate analysis of the spectrum of the system. It also eliminates the phenomenon of relative convergence which is introduced by the truncation of the field expansions.

More detailed descriptions of presented analytical techniques can be found in the following papers: Polewski et al. (2004) which presents formulation for metallic, dielectric and ferrite cylinders, Lech & Mazur (2007) considering formulation for segments of cylinders and cylinders with conducting strips and Lech et al. (2006); Polewski et al. (2006) presenting formulation for pseudo-chiral cylinders.

2.2.2 Hybrid technique

In hybrid approach discrete FDFD and analytical solutions of Maxwell equations are used in region I and II, respectively. The tangential components of electric and magnetic fields defined on surface $\mathcal{S}$ in region I can be expressed as follows:

$$E_t^I(\alpha = R, \beta, \gamma) = \sum_{n=-\infty}^{\infty} \sum_{m=-\infty}^{\infty} C_{nm} f_m^{\beta}(\beta) f_n^{\gamma}(\gamma), \tag{29}$$

$$H_t^I(\alpha = R, \beta, \gamma) = \sum_{n=-\infty}^{\infty} \sum_{m=-\infty}^{\infty} D_{nm} f_m^{\beta}(\beta) f_n^{\gamma}(\gamma), \tag{30}$$

where C_{mn} and D_{mn} are the unknown expansion field coefficients of electric and magnetic fields. In above equations $f_m^{\beta}(\beta)$ and $f_n^{\gamma}(\gamma)$ are the eigenfunctions which determines the variation of the field in the tangential to the surface $\mathcal{S}$ directions.
First stage of the analysis is to determine an impedance matrix **Z** which relates unknown electric (29) and magnetic (30) field coefficients and is defined as follows:

$$\mathbf{C} = \mathbf{ZD}, \tag{31}$$

where **C** and **D** are column vectors of C_{mn} and D_{mn} coefficients. In order to determine the **Z**-matrix the discrete finite-difference frequency-domain (FDFD) technique is used. In our considerations we focused on two group of objects presented in Fig. 10. The first group,

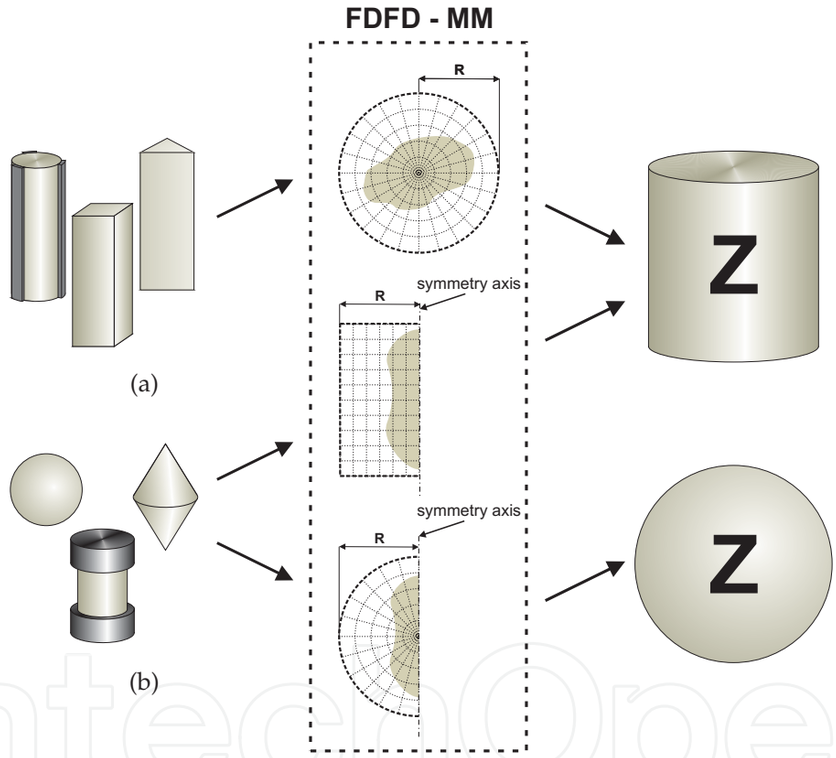

Fig. 10. Determination of Z-matrix with the use of hybrid FDFD-MM technique

presented in Fig. 10(a), includes cylinders homogenous along their height with arbitrary cross-section. The second group includes the axially-symmetrical posts with irregular shape (see Fig. 10(b)). The geometry properties of this objects allow one to simplify the three-dimensional (3D) problem to two-and-a-half dimensional (2.5D) one. As a result the investigated post is discretized only in the $\alpha - \beta$ or $\alpha - \gamma$ plane, while in the γ or β direction we assume analytical form of the fields which is determined by the series of eigenfunctions $f_n^{\gamma}(\gamma)$ or $f_m^{\beta}(\beta)$, respectively.
When the **Z**-matrix of the object is calculated we can treat the considered post with irregular shape as a homogenous cylinder or sphere with the boundary conditions defined by its impedance matrix. Now, imposing the boundary continuity conditions between tangential

components of fields in the outer (defined by equations (4) and (5)) and inner region (defined by equations (29) and (30)) we are obtaining **T**-matrix of analyzed object. More detailed description of the hybrid FDFD-MM method formulated in cylindrical and spherical coordinates is presented in Kusiek & Mazur (2009; 2010; 2011).

3. Applications

The investigation of electromagnetic wave scattering in inner region led us to the description of the analyzed set of objects by an aggregated $\overline{\overline{\mathbf{T}}}$-matrix defined on the surface $\mathcal{S}$ which surrounds the whole set. As the surface $\mathcal{S}$ is either cylindrical with circular cross-section or spherical the investigated structure is seen from a point of view of an incoming field in outer region as a simple cylinder or sphere with the boundary condition included in $\overline{\overline{\mathbf{T}}}$-matrix.
The outer region can be assumed as closed or open space allowing to analyze a wide group of application such as a rectangular waveguide junction, an open space with arbitrary incident plane wave, a circular waveguide or resonator. The aim of the analysis is to match the fields coming from the outer and the inner regions and formulate the generalized scattering matrix in closed structures and the scattering coefficients for the open structures.
In order to verify the obtained mathematical models of electromagnetic wave scattering a few configurations of the investigated structures in closed and open structures have been investigated. The results have been compared with those obtained from commercial simulators, found in literature and the author's experiment.

3.1 Waveguide resonators, filters and periodic structures

For the closed structures the outer region is assumed as the waveguide junction or resonator. The chosen applications to be investigated concern placing the circular inner region with a set of analyzed posts in a rectangular waveguide junction or limiting the circular inner region by electric walls forming a circular resonator. As a result of the closed structure investigation a multimode scattering matrix of a junction or a set of resonance frequencies of a cavity are obtained.
The first investigated configuration is a circular cavity resonator loaded with square dielectric cylinder. In the analysis an additional boundary conditions needed to be applied for the side wall of the cavity to obtain resonance frequencies. In the resonator case the Sommerfeld's radiation condition does not need to be satisfied, thus, for the numerical efficiency it is more convenient to replace the Hankel function of the second kind in the ρ-dependent field eigenfunctions in region outside the post with Bessel function of the second kind. This will ensure the values of resultant resonance frequencies of the cavity are real. For the chosen example the resonant frequencies calculated for different values of post displacement are presented in Table 1 and are compared with measurement. The obtained results show that by utilizing proposed method, a very good agreement with the measurements can be obtained.
By cascading single sections it is possible to utilize the presented method for filter or periodic structure design. In order to test the validity of the method the filter structure proposed in Alessandri et al. (2003) was investigated. The performance of the filter is predicted by cascading S-matrices of the separated sections. The results show again that utilizing this method a good agreement with calculations of the alternative numerical method was obtained. The possibility of applying this method to the investigation of other structures follows from the results.

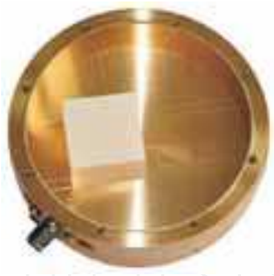

Table 1. Resonance frequencies (in GHz) of circular cavity resonator loaded with single square dielectric post: ($a = 20$mm, $\varepsilon_r = 11.25$) for different values of post shift d mm.

Mode	n	FDFD-MM			Measured	δ [%]
		$d = 15$	$d = 10$	$d = 0$	$d = 0$	
TM^1	0	1.7475	1.6299	1.5553	1.5568	0.10
TM^2	0	3.2373	3.1275	3.0646	3.0644	0.01
TM^3	0	3.2969	3.1375			
$hybrid^1$	1	4.0254	4.0305	4.0302	4.0056	0.61
$hybrid^2$	1	4.0556	4.0343			
TM^4	0	4.6021	4.4715	4.4229	4.4181	0.11
TM^5	0	4.7434	4.7523	4.7494	4.75	0.01

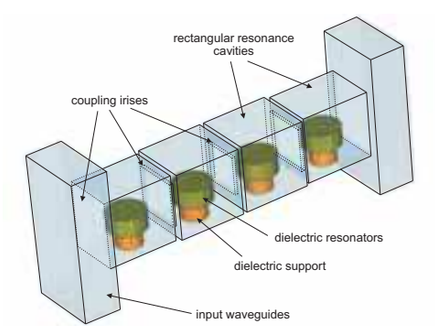

(a)

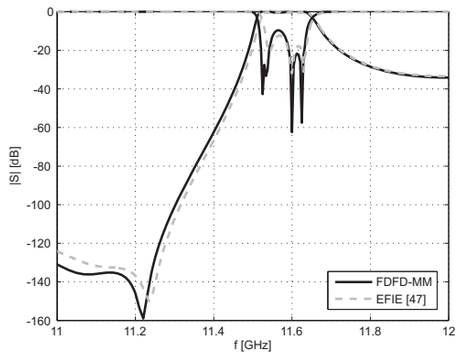

(b)

Fig. 11. Waveguide filter presented in Alessandri et al. (2003): (a) schematic view of the structure and (b) frequency response (input waveguides: 19.05×9.52mm, resonance cavities: $6.91 \times 9 \times 9$mm, $7.93 \times 9 \times 9$mm, coupling irises: $6.91 \times 9 \times 0.5$mm, $5.93 \times 5.86 \times 0.5$mm, $4.85 \times 5.25 \times 0.5$mm, dielectric resonators: $r = 2.53$mm, $h = 2.3$mm, $\varepsilon_r = 30$, dielectric support: $r = 1.75$mm, $h = 2.31$mm, $\varepsilon_r = 9$).

It was seen from the numerical results the post with arbitrary cross-section, as distinct from common cylinders, enables to vary the resonant frequency by a simple rotation of the object. In cascade filters with several posts, their rotation and shift influence the coupling between the filter resonators, which enables tuning of the circuit to the demanded frequency. The changes of a single post position affect the shift of the resonance frequency more than the rotation of the post. Changes of the post positions in the cascade affect the coupling values between the posts more and thereby introduce more perturbation to the resultant frequency response characteristic of the filter. The influence which the rotation of the post has on the resonance frequency can be used in cascade filter structures only to introduce slight adjustments to the filter frequency response. This effect permits us to compensate for material defects and improper dimensions or other mechanical inaccuracies of the structure which have an effect on the length of the cavities. The other advantage of using the nonhomogeneous cross-section of the resonators in filter structures is that there is no need to introduce additional tuning elements which would require some design modifications. The example of such filter is presented in Fig. 12.

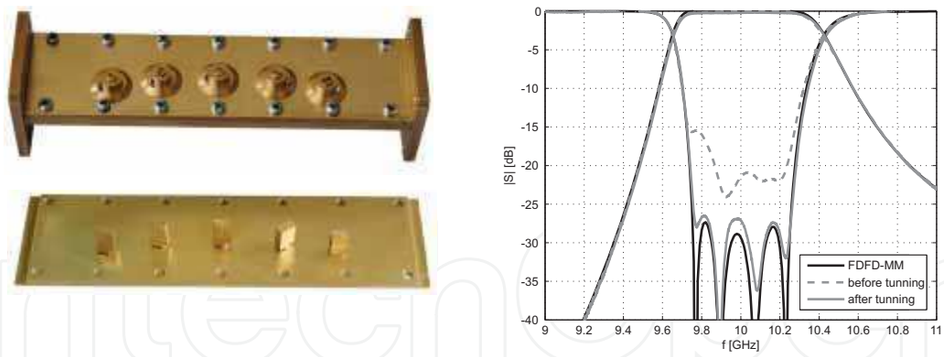

(a) (b)

Fig. 12. Waveguide direct coupled filter with rectangular posts: (a) photo of the fabricated structure and (b) simulated and measured frequency response (posts dimensions: 3×6mm and location: $l_1 = 18.31$mm, $l_2 = 21.31$mm, $d_1 = 5.76$mm, $d_2 = 3$mm, $d_3 = 2.37$mm). Waveguide dimensions: 22.86×10.16mm.

As can be seen the preliminary fabricated model with the post orientation identical to the designed filter did not give satisfactory agreement with the designed parameters. However, only slight corrections made by rotation of the post were needed to obtain the demanded shape of the frequency response characteristics. Despite the small discrepancies between the designed and measured patterns, the obtained results are more then satisfactory and, thanks to tuning ability provided by the applied rectangular posts, the design goal was accomplished proving the correctness of the approach.
The last analyzed structure presented in Fig. 13 is a waveguide filled with dielectric material ($\varepsilon_r = 2$) and loaded periodically with metallic circular cylinders of finite height. At first the

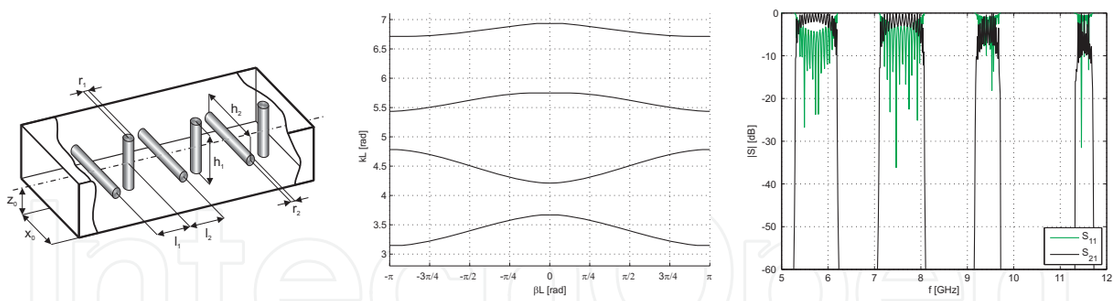

(a) (b) (c)

Fig. 13. Rectangular waveguide loaded periodically with metallic finite height circular cylinders: (a) view of the structure, (b) $k - \beta$ diagram and scattering parameters of pseudo-periodic structures composed of (c) twenty sections. Parameters of the structure: waveguide: 22.86×10.16mm, waveguide filling: $\varepsilon_r = 2$, $\mu_r = 1$, metallic cylinders: $r_1 = r_2 = 1$mm, $h_1 = h_2 = 8$mm, $x_0 = 11.43$mm, $z_0 = 5.08$mm, $l_1 = l_2 = 20$mm, single section length: $L = l_1 + l_2$.

dispersion diagram was determined for the investigated periodic structure (see Fig. 13(b)). This figure represents the plot of propagation coefficient βL as a function of kL. The results presented in $kL - \beta L$ diagrams clearly show passbands and stopbands formed in the periodic structure.

The scattering parameters for the finite periodic structures containing twenty sections of cylindrical posts were calculated and presented in Fig. 13(c). It is worth noticing that the bands shown in dispersion diagram for the infinite periodic structure are formed and are visible even for a finite periodic structure with small number of sections.

3.2 Antenna beam-forming structures

The method has been used to investigate open structures. Assuming the plane wave illumination it is possible to calculate the scattering coefficients and thus obtain scattered field pattern in near and far zones.

The rotation of the nonhomogeneous posts located in free space and illuminated by a plane wave triggers the possibility of shaping the scattered patterns of the post arrays and allows for some adjustments to the characteristics, such as reduction of the back and side lobes.

The first example concerns an array of five dielectric circular cylinders loaded with metallic rectangular cylinders and illuminated by TM plane wave. The results for two different angles φ_0 of plane wave illumination are presented in Fig. 14. From the presented results it can be noticed that the far field pattern is modified by changing the plane wave illumination angle. When the plane wave angle of incidence is changed to $\varphi_0 = 45^\circ$ the four main lobe appears in scattered field characteristic. The results well agree with those obtained form the alternative method. The second investigated example concerns a configuration of linear array of three

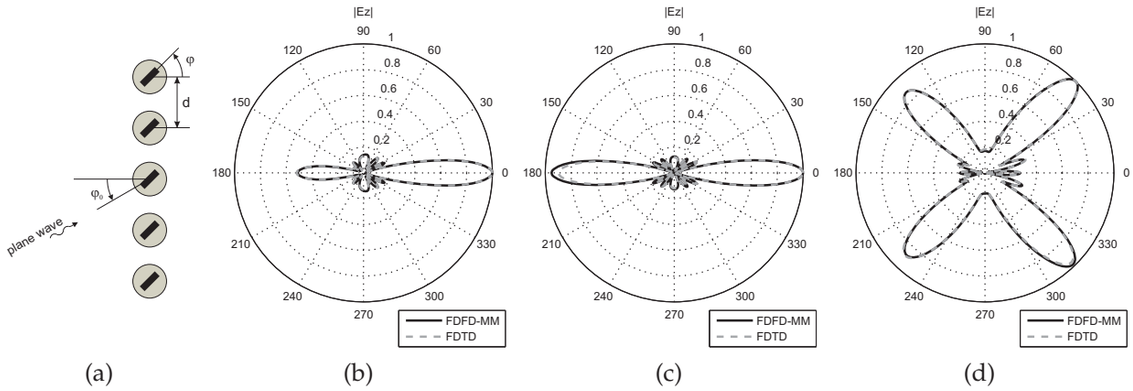

Fig. 14. Normalized amplitude of scattered z component of electric field for configuration of five dielectric circular cylinders ($\varepsilon_{ri} = 3$) loaded with rectangle metallic cylinders ($a_i = 0.2\lambda_0$, $b_i = 0.04\lambda_0$ for $i = 1, \ldots, 5$) for three different sets: (a) investigated structure and normalized scattered field patterns for: (b) $\varphi = 0$, $\varphi_0 = 0$, (c) $\varphi = 90^\circ$, $\varphi_0 = 0$, (d) $\varphi = 90^\circ$, $\varphi_0 = 45^\circ$.

Ω cylinders type '2'. The results are illustrated in Fig. 15. It is seen that the change of the sign of pseudochiral admittance Ω_c in the presented cases causes the reverse of the scattered field direction. Therefor, even thou the medium is isotropic, with the change of the sign of pseudochiral admittance Ω_c it is possible to obtain analogous effects as in the ferrite medium with the reverse of magnetization field.

The next investigated structure presented in Fig. 16 is a configuration of four dielectric cylinders illuminated by plane wave. The normalized scattered electric field pattern is presented in Figs. 16(b)-16(d). The results of proposed method well agree with the ones obtained from commercial software QuickWave 3D (FDTD). From the presented results it can be also noticed that the usage of the investigated dielectric posts allows to obtain the

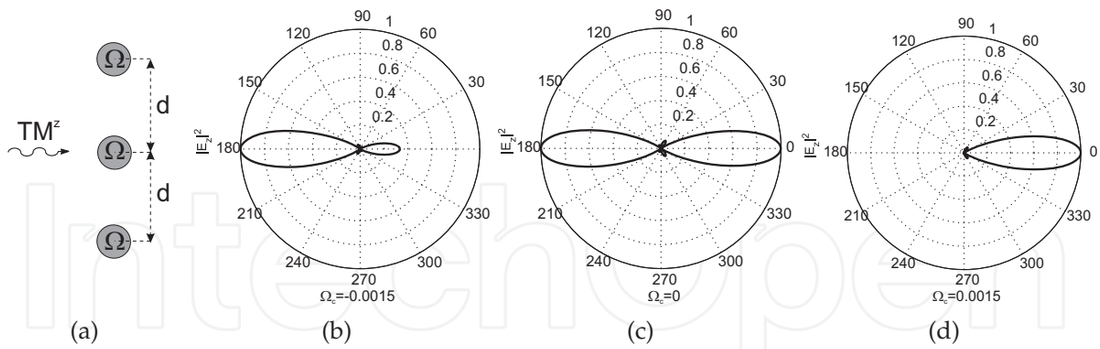

Fig. 15. Tipple post configuration ($f = 15GHz$, $r = 3mm$, $d = 10mm$, $\varepsilon_z = 4$, $\mu_\phi = 3.1$, $\mu = 1$): (a) investigated structure and normalized scattered field patterns for (b) $\Omega_c = -0.0015$ (c) $\Omega_c = 0$ and (d) $\Omega_c = 0.0015$

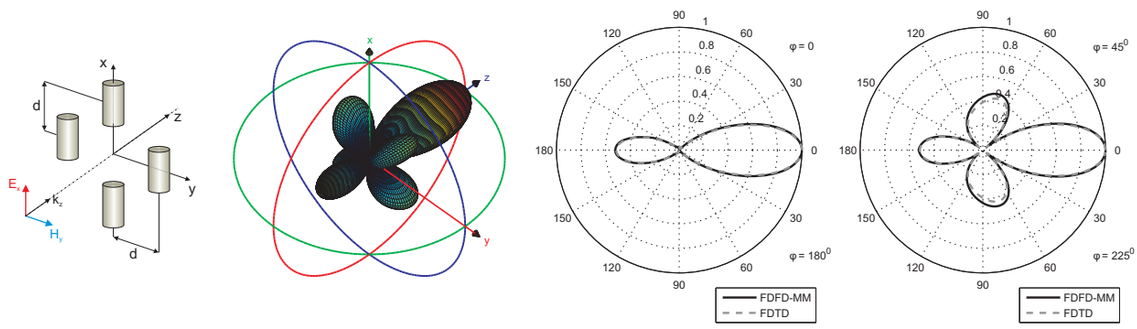

Fig. 16. Plane wave scattering on configuration of four dielectric cylinders: (a) investigated structure ($r = 3$mm, $h = 10$mm, $d = 12$mm, $\varepsilon_r = 5$, $f_0 = 14$GHz)), (b) normalized scattered electric field pattern and its cross-sections for (c) $\varphi = \{0, 180^\circ\}$ and (d) $\varphi = \{45^\circ, 225^\circ\}$ planes.

directional scattered field pattern with the low level of side lobes. This property of dielectric objects can be applied in antenna beam focusing systems.
The last structure is an array of sixteen metallic cylinders presented in Fig. 17(a). As in the previous case the analyzed set of objects is illuminated by plane wave. The normalized energy characteristics of scattered field pattern for two different frequencies of analysis are presented in Figs. 17(b) and 17(c). It can be noticed that the periodically situated posts allows to transmit or reflect almost all the power of the incident wave for different frequencies. This effect can be used in periodic structures to obtain the frequency selective surfaces which has a wide range of applications in novel microwave systems.

3.3 Multilayered periodic structures - tunneling and electromagnetic curtain effects

In this section the scattering and tunneling properties of multilayered periodic arrangement composed of frequency selective surfaces (FSS) will be presented.

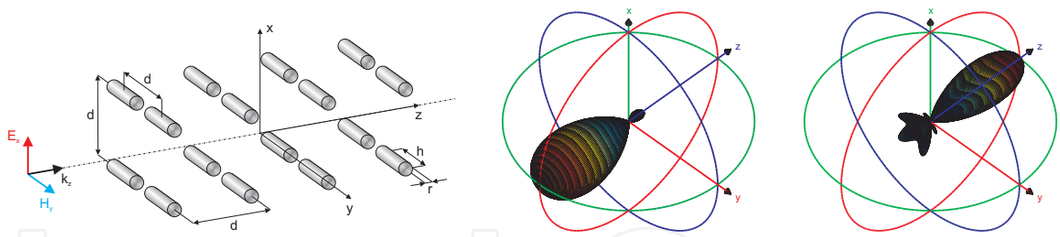

(a) (b) (c)

Fig. 17. Plane wave scattering by an array of sixteen metallic cylinders ($r = 2$mm, $h = 18$mm, $d = 16$mm): (a) investigated structure and normalized scattered power pattern and its cross-sections for (b) $f_0 = 5$GHz, and (c) $f_0 = 6$GHz

.

3.3.1 Description of the structure and methods of analysis

The structure under investigation is composed of a multilayered arrays of uniformly spaced identical sections situated in a free space and illuminated by a plane wave (see Fig. 18).

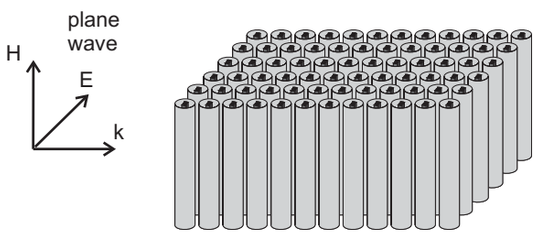

Fig. 18. Multilayered periodic structure composed of cylindrical objects

Such structures possess a stop band in their transmission characteristics and therefore are called electromagnetic band gap (EBG) structures in the microwave wavelength range. The constructive elements of these structures are comparable in size to the operation wavelength and may be composed of different media.

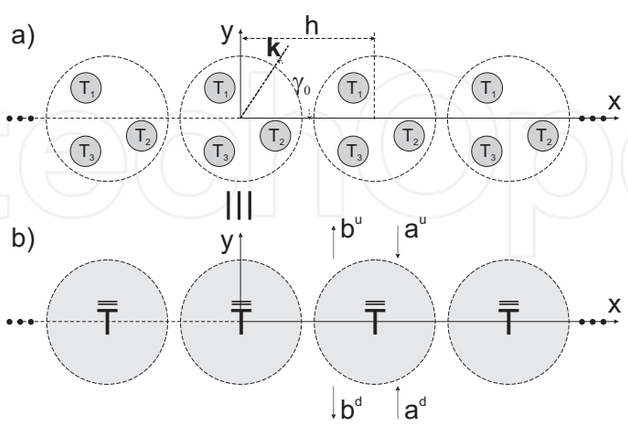

Fig. 19. Linear array of of uniformly spaced identical sections containing cylindrical objects described by their (a) **T**-matrix and (b) aggregated $\overline{\overline{\mathbf{T}}}$-matrix equivalent

The schematic representation of a single periodic array of cylindrical unit cells is presented in Fig. 19a. The unit cell contains cylindrical metallo-dielectric object or a set of objects each of

which is described by its isolated **T**-matrix. In case of multiple objects in a unit cell we use the ISP procedure to calculate the aggregated $\overline{\overline{\mathbf{T}}}$-matrix which then represents the whole unit cell as shown schematically in Fig. 19b. The aggregated $\overline{\overline{\mathbf{T}}}$-matrix is substantially changed by the geometric parameters of the posts such as dimension and location. For the single post located in the center of a unit cell the isolated **T**-matrix is utilized in the further analysis as a **T**-matrix of a whole unit cell. Thus, in both cases the investigation boils down to plane wave scattering from a periodic array of cylinders (unit cells), each of which is characterized by the aggregated $\overline{\overline{\mathbf{T}}}$-matrix.

It is assumed in the analysis that the investigated periodic array of cylinders is situated in a free space and the cylinders are infinitely long, parallel to each other and spaced with distance h along x axis on the plane $y = 0$. The direction of electromagnetic plane wave incidence is assumed to be normal to the cylinder axis. The electric or magnetic field vector of an incident plane wave may be slanted with respect to the post axis, but with the above assumptions the problem is reduced to a two-dimensional one and therefore the incident polarization may be decomposed into the two fundamental polarizations: TM and TE relative to the z axis.

In order to calculate a multimodal scattering matrix of a periodic array of cylindrical scatterers we utilize an efficient numerical technique described in Kushta & Yasumoto (2000) which is based on the transmission matrix approach and uses the lattice sums technique Yasumoto & Yoshitomi (1999). In this method the scattering matrix which relates the incident space-harmonics to the scattered, both reflected and transmitted ones, is defined for a periodic array. The scattering matrix is expressed in terms of lattice sums characterizing a periodic arrangement of scatterers and the aggregated $\overline{\overline{\mathbf{T}}}$-matrix for posts located within a unit cell.

Having obtained the scattering matrix of a single periodic array of cylindrical objects one can investigate the N-layered periodic array as shown in Fig. 20. The cylindrical sections in different layers need not be identical, i.e. the dimensions, the material parameters and the arrangement of the posts in the unit cell can be arbitrary for different layers. These differences will affect the aggregated $\overline{\overline{\mathbf{T}}}$-matrix of the unit cell. Additionally, the period between the cells in different layers can also be arbitrary, which will in turn require calculating different lattice sums for each layer. For the sake of generalization, the spacing between layers can also be chosen arbitrarily.

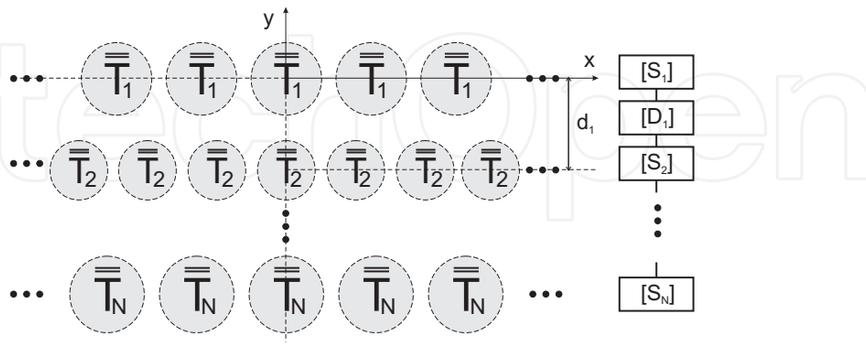

Fig. 20. Cross section of a square lattice periodic array of cylindrical sections described by aggregated $\overline{\overline{\mathbf{T}}}$-matrix

In our approach, instead of utilizing a popular recursive formula Yasumoto (2000) for analyzing multilayered periodic arrays, we calculate the scattering matrix of N-layered

structure by cascading the scattering matrices of each periodic array and the scattering matrices of free space, defined utilizing the decaying space harmonic components, which include the spacing between the layers (see Fig. 20). To calculate the scattering matrix of the entire structure we utilize the formula for cascading discontinuities described by their **S**-matrices presented in Uher et al. (1993).

3.3.2 Results

A few examples of multilayered periodic structures have been analyzed and the reflection characteristics of these arrays have been calculated. The results are shown for the wavelength range $h/\lambda_0 < 1$ under normal incidence, as only for such a situation the use of periodic arrays as frequency and polarization selective components fulfils its function. Only the fundamental Floquet mode $\nu = 0$ is propagating in this range, thus the characteristics are plotted for R_0 denoting the reflection coefficient of the fundamental space harmonic.

Although the fundamental mode is the only one propagating in the investigated range, the analysis of multilayered systems demands utilizing the multimodal scattering matrix of a single periodic array in the cascading process. The importance of this fact is depicted in the first example proposed in Yasumoto et al. (2004). The power reflectance R_0 for the structure composed of two identical arrays of dielectric cylinders is calculated utilizing the cascading procedure with the evanescent space harmonics neglected in the analysis, and the results are presented in Fig. 21a. The scattering matrices of both periodic arrays were of the dimensions 2×2 and contain only the reflection and transmission parameters of the fundamental mode. As can be seen from the results, a single peak appeared in the wavelength response of the double-layered system for both TM and TE polarizations. However, calculating the same system as a one-layered periodic array of cylindrical sections containing two dielectric cylinders per section, one obtains the wavelength response in reflection coefficient as depicted in Fig. 21b. In this case, the aggregate $\overline{\overline{\mathbf{T}}}$-matrix of a single section in the array was calculated utilizing the ISP. Comparing the results, one can see considerable differences in the wavelength responses. Calculating the system again as two-layered periodic structure of circular dielectric cylinders, but taking into account the higher evanescent space harmonics, one obtains the wavelength responses depicted in Fig. 21c. The results coincide with those from Fig. 21b, which shows that the evanescent space harmonics play an important role in wavelength response of multilayered arrays and the presented simplifications lead to erroneous results in the scattering characteristics of the system. The results are with an excellent agreement with those presented in Yasumoto et al. (2004), where the recursive algorithm for the generalized reflection matrix was used for calculation of the periodic system.

3.3.3 Electromagnetic curtain effect

In a layered system, the multiple interaction of space harmonics scattered from each of the array layers modifies the frequency response, and bandgaps or stopbands in which any electromagnetic wave propagation is forbidden are formed. The power reflection coefficients for one-hundred-layered square lattice periodic arrays with one strip-metallized post embedded in a dielectric cylinder per unit cell versus frequency are illustrated in Figs. 23 for normal incidence of TM and TE waves. Each figure consists of three characteristics for different rotation angles of the posts. For both polarizations a single stop band is chosen and depicted in the figure. It is noticeable that for rotation angle $\xi = 90^\circ$ stop bands for both polarizations are formed in the same frequency range. The characteristic plotted for TE wave is insensitive on the posts rotation angle, however the stop band width for TM

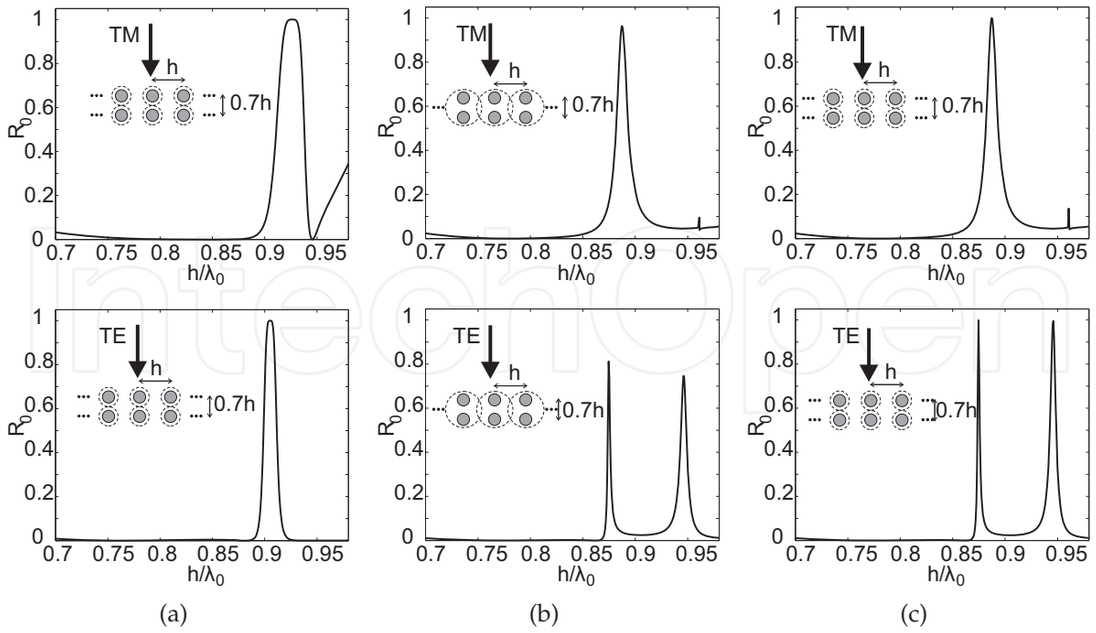

Fig. 21. Power reflection coefficients of the fundamental space harmonics versus non-dimensional frequency h/λ_0 for normal incidence of TM and TE waves into two-layered periodic structure of circular dielectric cylinders. Parameters of the post: $r = 0.3h$, $\varepsilon_r = 2$. (a) results obtained without the inclusion of evanescent space-harmonics, (b) results calculated for single periodic array of double cylinder configuration (ISP procedure) and (c) results obtained with the inclusion of evanescent space-harmonics

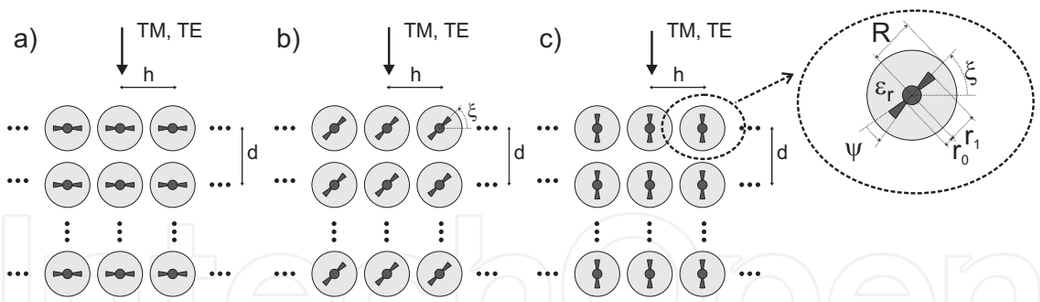

Fig. 22. Cross section of a square lattice periodic array of metallized cylindrical objects for different ξ angles: a) $\xi = 0°$, b) $\xi = 45°$, c) $\xi = 90°$

wave is gradually narrowing with the posts rotating from $\xi = 90°$ to $\xi = 0°$ and almost vanishes for the latter. The effect described above can be called an electromagnetic curtain effect, which allows to control the transmission of TM polarized wave though the periodic structure, while TE wave is blocked. A similar effect was obtained and presented in Toyama & Yasumoto (2005) in the case of a periodic array of composite circular dielectric cylinders with two cylindrical inclusions, only in that case stop bands for both TE and TM wave polarizations were narrowing and did not vanish in any case.

Another interesting case of band shifting can be observed for the structures with the whole layers rotated with respect to each other. In the example presented in Fig. 24 both EBG

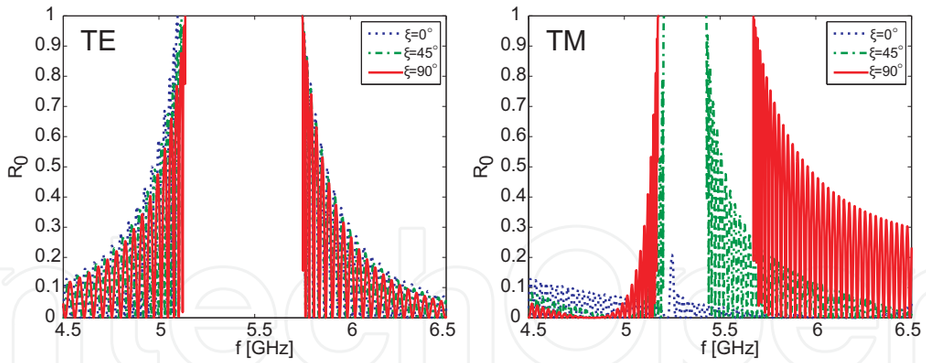

Fig. 23. Power reflection coefficients of the fundamental space harmonics versus frequency for one-hundred-layered square lattice periodic arrays of metallic posts embedded in dielectric cylinders from Fig 22. Parameters of the structure: $h = 19.5$mm, $d = 25$mm, $r_0 = 0.01h$, $r_1 = 0.09h$, $R = 0.19h$, $\psi_{1,2} = 10^\circ$, $\varepsilon_r = 20$

structures are identical but rotated by 90° with respect to each other. For the same plane wave illuminating both configurations, they produce stop bands which only slightly overlap. When half of the structure (i.e. 10 last or first arrays) are being rotated with respect to the other half one obtains the effect of stop band shifting. The stop bands, which are almost identical in width, can be shifted from one bandwidth to another. The case of 90° rotation of stacks is presented in Fig. 24(b). When only every other periodic array are being rotated the produced stop band is widening and in the case of 90° rotation it embraces both stop bands as can be seen in Fig. 24(c).

3.3.4 Tunneling effect

An interesting effect of wave tunneling can be obtained in the structure under investigation. This effect, along with the "growing evanescent envelope" for field distributions, was previously observed in metamaterial medium (negative value of real permittivity and permeability) and a structure composed of a pair of only-epsilon-negative and only-mu-negative layers Alu & Engheta (2003). This effect was also discussed in Alu & Engheta (2005) for periodically layered stacks of frequency selective surfaces (FSS). It was shown in Alu & Engheta (2005) that a complete electromagnetic wave tunneling may be achieved through a pair of different stacked FSSs which are characterized by dual behaviors, even though each stack is completely alone opaque (operates in its stop band).

Similar effect can be obtained for the structure composed of a pair of identical stacks of periodic arrays of cylindrical posts rotated by 90° with respect to each other. This effect can also be controlled by introducing a gap d between the stacks (see Fig. 25). The calculation of a total scattering matrix for a pair of such stacks boils down to cascading the scattering matrix of a stack calculated for TE wave excitation with the scattering matrix calculated for TM wave excitation.

The tunneling effect has been obtained for the periodic structure described in Fig. 25. The stop bands are formed in the same frequency range for both TE and TM waves. Therefore, we obtain a pair of stacks with dual behavior both of which operate in their stop bands. In the equivalent circuit analogy one stack is represented by a periodical line loaded with capacitors, while the other one is loaded with inductances.

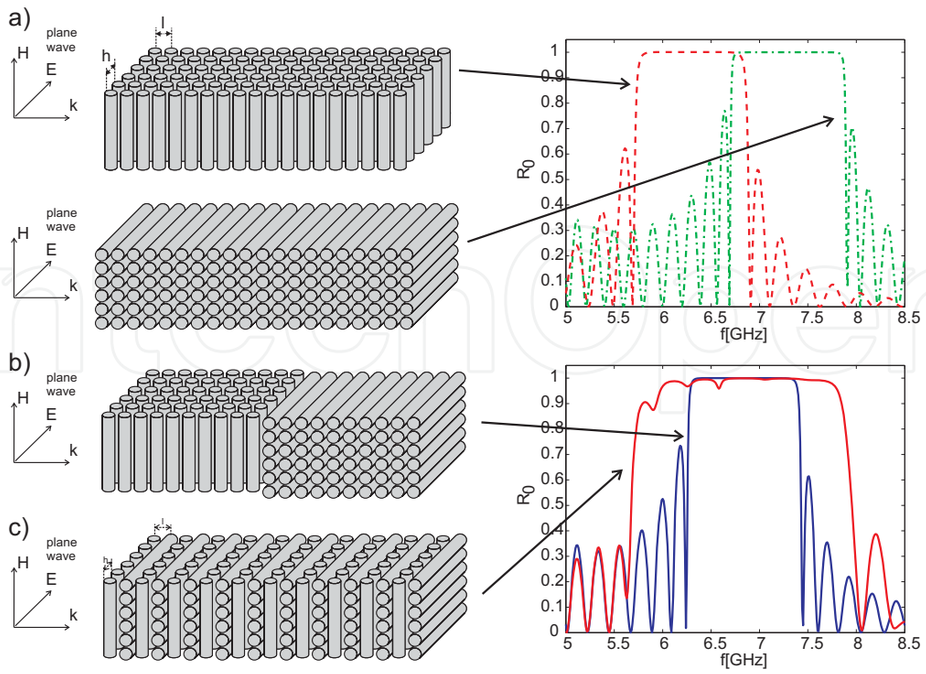

Fig. 24. Power reflection coefficients of the fundamental space harmonics versus frequency for normal incidence of TE wave on a periodic structures; Parameters of the structures $h = 20\text{mm}$, $l = h$, $r = 0.06h$, $R = 0.35h$, $\varepsilon_{r1} = 3$, $\varepsilon_{r2} = 2.5$, number of sections 20.

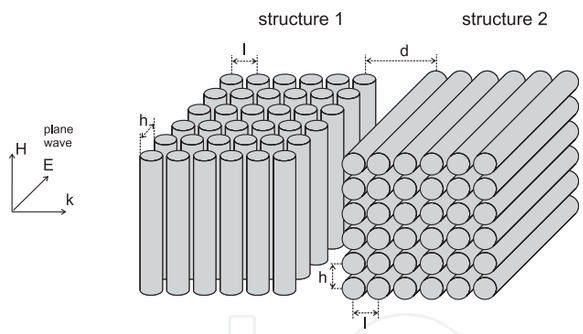

Fig. 25. Schematic 3-D representation of a periodic structure under investigation

Fig. 26 illustrates the power reflection coefficients for the normal incidence of a TE polarized plane wave on stacks of periodic structures of dielectric cylinders with double dielectric inclusions. The characteristics for scattering from structure 1, 2 and 3 are illustrated. The results show that stacks 1 and 2 are completely opaque in presented frequency ranges. However, when half of these configurations are rotated by 90° with respect to the other half, forming the structure 3, the tunneling effect can be observed. The obtained configurations enable the signal from a very narrow frequency range to tunnel through the structure.
This tunneling effect can be controlled by adjusting the distance d between stacks (see Fig. 25). Fig. 27 shows the characteristics of the power reflection coefficients for the normal incidence of a TE polarized plane wave on structure 3 for different values of distance d. It can be clearly seen that this value is directly connected to the frequency of the tunneled wave.

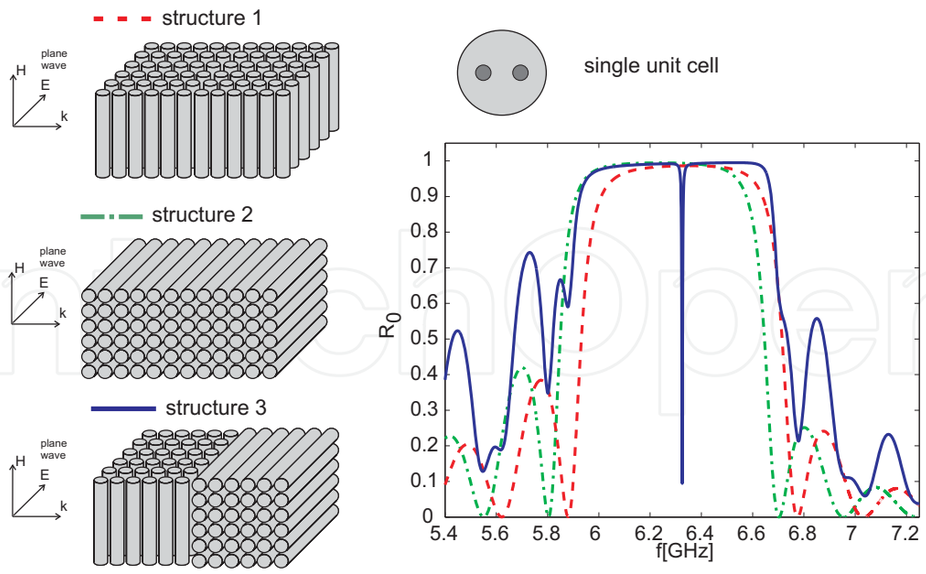

Fig. 26. Power reflection coefficients of the fundamental space harmonics versus frequency for normal incidence of TE wave on a periodic structures; Parameters of the structures: $h = 20$mm, $l = 20$mm, $d = l$, $R = 0.48h$, $\varepsilon_r = 1.5$, inclusion - two dielectric cylinders $r = 0.16h$, $\varepsilon_{rc} = 2$, displacement from the center $.24h$ number of sections 20;

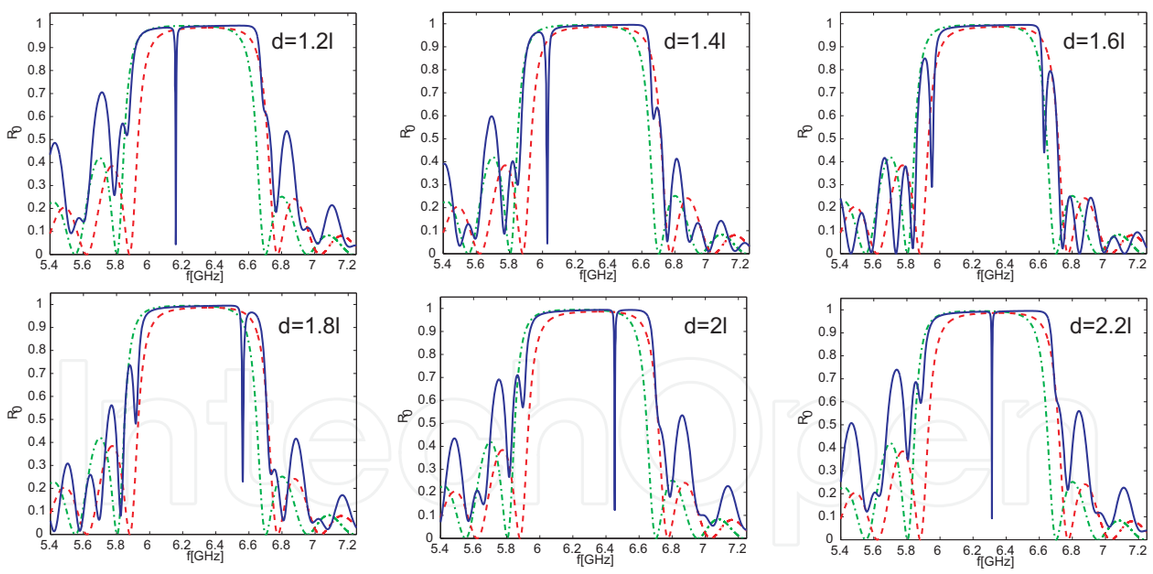

Fig. 27. Power reflection coefficients of the fundamental space harmonics versus frequency for normal incidence of TE wave on a periodic structures described in Fig. 26 for different values of distance d between stacks; dashed line (red) - structure 1, dash-dot line (green) - structure 2; solid line (blue) - structure 3

4. Conclusion

In the chapter a hybrid method of electromagnetic wave scattering from structures containing complex cylindrical or spherical objects is presented. Depending of the investigated post geometry different numerical techniques were utilized such as mode-matching technique, method of moments and finite difference method defined in the frequency domain. The proposed approach enables to determine the scattering parameters of open and closed structures containing the configuration of cylindrical objects of arbitrary cross-section and axially symmetrical posts. The proposed technique rests on defining the collateral cylindrical or spherical object containing the investigated element and then utilizing the analytical iterative model for determining scattering parameters of arbitrary configuration of objects. The obtained solution can be combined with the arbitrary external excitation which allows analyzing the variety of open and closed microwave structures. The convergence of the method have been analyzed during the numerical studies. Additionally, in order to verify the correctness of the developed method the research of a number of open and closed microwave structures such as beam shaping configurations, resonators, filters and periodic structures have been conducted. The obtained numerical results have been verified by comparing them with the ones obtained form alternative numerical methods or own measurements. A good agreement between obtained results was achieved.

5. Acknowledgement

This work was supported in part by the Polish Ministry of Science and Higher Education under Contract N515 501740, decision No 5017/B/T02/2011/40 and in part from sources for science in the years 2010-2012 under COST Action IC0803, decision No 618/N-COST/09/2010/0.

6. References

Aiello, G., Alfonzetti, S. & Dilettoso, E. (2003). Finite-element solution of eddy-current problems in unbounded domains by means of the hybrid FEM-DBCI method, *MAGN* 39(3): 1409 – 1412.

Alessandri, F., Giordano, M., Guglielmi, M., Martirano, G. & Vitulli, F. (2003). A new multiple-tuned six-port Riblet-type directional coupler in rectangular waveguide, *IEEE Trans. Microw. Theory Tech.* 51(5): 1441 – 1448.

Alu, A. & Engheta, N. (2003). Pairing an epsilon-negative slab with a mu-negative slab: Resonance, tunneling and transparency, *IEEE Trans. Antennas Propag.* 51(10): 2558–2571.

Alu, A. & Engheta, N. (2005). Evanescent growth and tunneling through stacks of frequency-selective surfaces, *IEEE Antennas Wireless Propag. Letters* 4: 417–420.

Arndt, F., Catina, V. & Brandt, J. (2004). Efficient hybrid MM/MoM technique for the CAD of circular combline filters with resonators of more general shape, *IEEE Microwave Symposium Digest* 3: 1407 – 1410.

Aza, G., Encinar, J. A., Zapata, J. & Lambea, M. (1998). Full-wave analysis of cavity-backed and probe-fed microstrip patch arrays by a hybrid mode-matching generalized scattering matrix and finite-element method, *IEEE Trans. Antennas Propag.* 46(2): 234 – 242.

Dittloff, J., Arndt, F. & Grauerholz, D. (1988). Optimum design of waveguide E-plane stub-loaded phase shifters, *IEEE Trans. Microw. Theory Tech.* 36(3): 582–587.

Elsherbeni, A. Z., Hamid, M. & Tian, G. (1993). Iterative scattering of a Gaussian beam by an array of circular conducting and dielectric cylinders, *J. of Electromag. Waves App.* 7(10): 1323–1342.

Esteban, H., Cogollos, S., Boria, V., Blas, A. S. & Ferrando, M. (2002). A new hybrid mode-matching/numerical method for the analysis of arbitrarily shaped inductive obstacles and discontinuities in rectangular waveguides, *IEEE Trans. Microw. Theory Tech.* 50(4): 1219–1224.

Gimeno, B., Cruz, J. L., Navarro, E. A. & Such, V. (1994). A polarizer rotator system for three-dimensional oblique incidence, *IEEE Trans. Antennas Propag.* 42(7): 912–919.

Hamid, A.-K., Ciric, I. & Hamid, M. (1991). Iterative solution of the scattering by an arbitrary configuration of conducting or dielectric spheres, *IEE Proc. H Microw., Antennas Propag.* 138(6): 565 – 572.

Kildal, P.-S., Kishk, A. A. & Tengs, A. (1996). Reduction of forward scattering from cylindrical objects using hard surfaces, *IEEE Trans. Antennas Propag.* 44: 1509–1520.

Kushta, T. & Yasumoto, K. (2000). Electromagnetic scattering from periodic arrays of two circular cylinders per unit cell, *Prog. Electromag. Research* 29: 69–85.

Kusiek, A. & Mazur, J. (2009). Analysis of scattering from arbitrary configuration of cylindrical objects using hybrid finite-difference mode-matching method, *Prog. Electromag. Research* 97: 105 – 127.

Kusiek, A. & Mazur, J. (2010). Hybrid finite-difference/mode-matching method for analysis of scattering from arbitrary configuration of rotationally-symmetrical posts, *Prog. Electromag. Research* 110: 23 – 42.

Kusiek, A. & Mazur, J. (2011). Application of hybrid finite-difference mode-matching method to analysis of structures loaded with axially-symmetrical posts, *Microw. Opt. Tech. Lett.* 53(1): 189–194.

Lech, R. & Mazur, J. (2007). Analysis of circular cavity with cylindrical objects, *IEEE Trans. Microw. Theory Tech.* 55(10): 2115 – 2123.

Lech, R., Polewski, M. & Mazur, J. (2006). Electromagnetic wave scattering by a set of axially symmetric ω-medium cylinder, *Microw. Opt. Tech. Lett.* 48(9): 1880 – 1884.

Mrozowski, M. (1994). A hybrid PEE-FDTD algorithm for accelerated time domain analysis of electromagnetic waves, *IEEE Microw. Guided Wave Lett.* 4: 323 – 325.

Mrozowski, M., Okoniewski, M. & Stuchly, M. (1996). A hybrid PEE-FDTD method for efficient field modeling in cyllindrical coordinates, *Elect. Lett.* 32: 194 – 195.

Polewski, M., Lech, R. & Mazur, J. (2004). Rigorous modal analysis of structures containing inhomogeneous dielectric cylinders, *IEEE Trans. Microw. Theory Tech.* 52(5): 1508–1516.

Polewski, M., Lech, R. & Mazur, J. (2006). Radiation phenomena from pseudochiral cylinders at plane wave incidence, *Microw. Opt. Tech. Lett.* 48(9): 1880 – 1884.

Polewski, M. & Mazur, J. (2002). Scattering by an array of conducting lossy dielectric, ferrite and pseudochiral cylinders, *Prog. Electromag. Research* pp. 283–310.

Quick Wave 3D (QWED) (n.d.). http://www.qwed.com.pl/.

Rogier, H. (1998). A new hybrid FDTD-BIE approach to model electromagnetic scattering problems, *IEEE Microw. Guided Wave Lett.* 8(3): 138 – 140.

Roy, T., Sarkar, T. K., DjordjeviC, A. R. & Salazar-Palma, M. (1996). A hybrid method solution of scattering by conducting cylinders (TM case), *IEEE Trans. Microw. Theory Tech.* 44(12): 2145 – 2151.

Rubio, J., Arroyo, J. & Zapata, J. (1999). Analysis of passive microwave circuits by using a hybrid 2-D and 3-D finite-element mode-matching method, *IEEE Trans. Microw. Theory Tech.* 47(9): 1746 – 1749.

Sabbagh, M. E. & Zaki, K. (2001). Modeling of rectangular waveguide junctions containing cylindrical posts, *Prog. Electromag. Research* 33: 299–331.

Sharkawy, M. A., Demir, V. & Elsherbeni, A. Z. (2006). Plane wave scattering from three dimensional multiple objects using the iterative multiregion technique based on the FDFD method, *IEEE Trans. Antennas Propag.* 54(2): 666–673.

Shen, T., Zaki, K. A. & Wang, C. (2000). Tunable dielectric resonators with dielectric tuning disks, *IEEE Trans. Microw. Theory Tech.* 48: 2439Ű2445.

Toyama, H. & Yasumoto, K. (2005). Electromagnetic scattering from periodic arrays of composite circular cylinder with internal cylindrical scatterers, *Prog. Electromag. Research* 52: 355–358.

Uher, J., Bornemann, J. & Rosenberg, U. (1993). *Waveguide Components for Antenna Feed Systems: Theory and CAD*, Artech House Antennas and Propagation Library, Norwood.

Waterman, P. C. (1971). Symmetry, unitarity and geometry in electromagnetic scattering, *Physical Review D* 3: 825–839.

Xu, F. & Hong, W. (2004). Analysis of two dimensions sparse multicylinder scattering problem using DD-FDTD method, *IEEE Trans. Antennas Propag.* 52(10): 2612 – 2617.

Yasumoto, K. (2000). Generalized method for electromagnetic scattering by two-dimensional periodic discrete composites using lattice sums, *Proc. Int. Conf. Microwave and Millimeter Wave Technology* (9): 29–34.

Yasumoto, K., Toyama, H. & Kushta, T. (2004). Accurate analysis of two-dimensional electromagnetic scattering from multilayered periodic arrays of circular cylinders using lattice sums technique, *IEEE Trans. Antennas Propag.* 52: 2603–2611.

Yasumoto, K. & Yoshitomi, K. (1999). Efficient calculation of lattice sums for freespace periodic green's function, *IEEE Trans. Antennas Propag.* 47(6): 1050–1055.

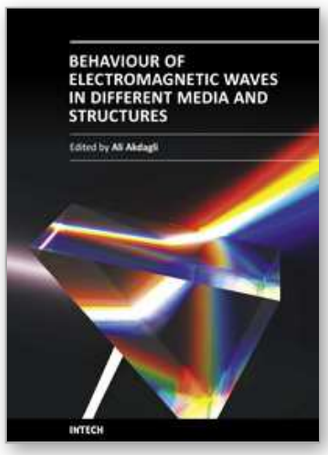

Behaviour of Electromagnetic Waves in Different Media and Structures

Edited by Prof. Ali Akdagli

ISBN 978-953-307-302-6
Hard cover, 440 pages
Publisher InTech
Published online 09, June, 2011
Published in print edition June, 2011

This comprehensive volume thoroughly covers wave propagation behaviors and computational techniques for electromagnetic waves in different complex media. The chapter authors describe powerful and sophisticated analytic and numerical methods to solve their specific electromagnetic problems for complex media and geometries as well. This book will be of interest to electromagnetics and microwave engineers, physicists and scientists.

How to reference

In order to correctly reference this scholarly work, feel free to copy and paste the following:

Adam Kusiek, Rafal Lech and Jerzy Mazur (2011). Electromagnetic Wave Scattering from Material Objects Using Hybrid Methods, Behaviour of Electromagnetic Waves in Different Media and Structures, Prof. Ali Akdagli (Ed.), ISBN: 978-953-307-302-6, InTech, Available from: http://www.intechopen.com/books/behavior-of-electromagnetic-waves-in-different-media-and-structures/electromagnetic-wave-scattering-from-material-objects-using-hybrid-methods2

INTECH
open science | open minds

InTech Europe
University Campus STeP Ri
Slavka Krautzeka 83/A
51000 Rijeka, Croatia
Phone: +385 (51) 770 447
Fax: +385 (51) 686 166
www.intechopen.com

InTech China
Unit 405, Office Block, Hotel Equatorial Shanghai
No.65, Yan An Road (West), Shanghai, 200040, China
中国上海市延安西路65号上海国际贵都大饭店办公楼405单元
Phone: +86-21-62489820
Fax: +86-21-62489821

IntechOpen